

## Research Article

# Photoacoustic Study of CdS QDs for Application in Quantum-Dot-Sensitized Solar Cells

S. Abdallah,<sup>1,2</sup> N. Al-Hosiny,<sup>1</sup> and Ali Badawi<sup>1,3</sup>

<sup>1</sup>Department of Physics, Taif University, Taif 21974, Saudi Arabia

<sup>2</sup>Department of Mathematical and Physical Engineering, Benha University, Benha 13511, Egypt

<sup>3</sup>Physics Department, Ain Shams University, Cairo 11566, Egypt

Correspondence should be addressed to S. Abdallah, dr.saidabdallah@yahoo.com

Received 11 April 2012; Accepted 8 September 2012

Academic Editor: Christian Brosseau

Copyright © 2012 S. Abdallah et al. This is an open access article distributed under the Creative Commons Attribution License, which permits unrestricted use, distribution, and reproduction in any medium, provided the original work is properly cited.

The optical properties and photovoltaic characterization of CdS quantum dots sensitized solar cells (QDSSCs) were studied. CdS QDs were prepared by the chemical solution deposition (CD) technique. Photoacoustic spectroscopy (PA) was employed to study the optical properties of the prepared samples. The sizes of the CdS QDs were estimated from transmission electron microscope (TEM) micrographs gives radii ranged from 1.57 to 1.92 nm. The current density-voltage ( $J$ - $V$ ) characteristic curves of the assembled QDSSCs were measured. Fluorine doped Tin Oxide (FTO) substrates were coated with 20 nm-diameter TiO<sub>2</sub> nanoparticles (NPs). Presynthesized colloidal CdS quantum dots of different particles size were deposited on the TiO<sub>2</sub>-coated substrates using direct adsorption (DA) method. The FTO counter electrodes were coated with platinum, while the electroelectrolyte containing  $I^-/I_3^-$  redox species was sandwiched between the two electrodes. The short current density ( $J_{sc}$ ) and efficiency ( $\eta$ ) increases as the particle size increases. The values of  $J_{sc}$  increases linearly with increasing the intensities of the sun light which indicates the greater sensitivity of the assembled cells.

## 1. Introduction

During the last two decades, there has been a great interest in material sciences for studying semiconducting quantum dots, since many of their physicochemical properties are substantially different from analogous properties of macroscopic solids [1]. Due to quantum confinement effect, they show size dependent optical, thermal, electrical, and photoluminescence properties. Particularly, II-VI semiconductor nanoparticles are currently of great interests for their practical applications in a variety of optoelectronic devices such as, high efficiency thin film transistors, light-emitting diodes [2], electron-beam pumped lasers, and electroluminescent devices [3–8]. CdS quantum dots (QDs) have become a very attractive promising material for many specific applications in solar energy conversion. Special attention has been devoted to investigate the optical and thermal properties to enhance the performance of solar cell devices. Generally, the absorption spectra can be measured by the conventional transmitted intensity method however; samples should be

sufficiently thin and have good quality surfaces by pre-treatments. This requires samples to be placed in a matrix of transparent material which on the other hand would interfere with the measurements of thermal properties [8]. Photoacoustic (PA) technique is proved to be useful for investigating the optical absorption of opaque samples as well as thermal properties of various materials by measuring the nonradioactive deexcitation processes [9, 10]. There are many methods used to anchor QDs onto the large band gap metal oxides. Normally, these adsorption methods are (1) *in situ* growth of QDs by either chemical bath deposition (CBD) technique [11–13], containing both the cationic and anionic precursors, or successive ionic layer adsorption and reaction deposition (SILAR) method [14–18], (2) *ex situ* growth as electrophoretic deposition (EPD) method [19, 20], linker-assisted adsorption (LA) [19, 21–23], and direct adsorption (DA) technique [22, 24, 25].

In this work we utilize PA spectroscopy to investigate the optical properties of CdS QDs. CdS QDs were synthesized by chemical deposition (CD) technique. The particles sizes were

then estimated using the transmission electron microscope (TEM). Furthermore, the presynthesized CdS QDs were adsorbed onto TiO<sub>2</sub> NPs by DA technique for different dipping times under ambient conditions. The effect of the CdS QDs size on the QDSSCs characteristic parameters (short circuit current density ( $J_{sc}$ ), open circuit voltage ( $V_{oc}$ ), fill factor (FF), and efficiency for energy conversion ( $\eta$ )) were studied.

## 2. Experiment

**2.1. Preparation of CdS Quantum Dots.** Spherical CdS colloidal nanocrystals were prepared by chemical deposition method according to a procedure reported elsewhere [26]. In this procedure, hexadecylamine (HAD) was used as a capping agent together with trioctylphosphine oxide (TOPO) and trioctylphosphine (TOP) to obtain size distribution less than 5%. The sulfur source such as sodium sulfide (Na<sub>2</sub>S) and dimethylcadmium were dissolved of trioctylphosphine (TOP) and rapidly injected into a vigorously stirred mixture of trioctylphosphine oxide (TOPO) and hexadecylamine (HDA). Four samples of different sizes were obtained from the same synthesis at four regular time intervals, during growth labelled (a–d).

**2.2. Preparation of Solar Cell Electrodes.** A colloidal paste of TiO<sub>2</sub> nanoparticles (NPs) was prepared by the method of Syrokostas et al. [27]. Three grams of commercial TiO<sub>2</sub> nanopowder (20 nm) (Degussa P-25 Titanium dioxide consists of 80% anatase and 20% rutile) was ground in a porcelain mortar and mixed with a small amount of distilled water (1 mL) containing acetyl acetone (10% v/v) to create the paste. Acetyl acetone was used as a dispersing agent. The paste was diluted further by slow addition of distilled water (4 mL) under continued grinding. Finally, a few drops of a detergent (Triton X-100) were added to facilitate the spreading of the paste on the substrate, since this substance has the ability to reduce surface tension, resulting in even spreading and reducing the formation of cracks. The TiO<sub>2</sub> paste was deposited on a conducting glass substrate of SnO<sub>2</sub>:F (FTO) with sheet resistance of 7  $\Omega$ /sq and >80% transmittance in the visible region, using a simple doctor blade technique. This was followed by annealing at 450°C for 30 min and the final thickness was 8  $\mu$ m after the solvent evaporation. Then the TiO<sub>2</sub> films were dipped into a colloidal solutions of presynthesized CdS QDs, for different dipping times (3, 6, 24, and 50 hours) to form four working electrodes. The counter electrodes were prepared by coating another FTO substrate sheet of resistance of 7  $\Omega$ /sq with Pt.

**2.3. Assembly of QDSSC.** Both of the working and counter electrodes were assembled as a sandwich type cell using clamps. Then they were sealed by using a hot-melt polymer sheet (solaronix, SX1170-25PF) of 25  $\mu$ m thickness in order to avoid evaporation of electrolyte. Finally, Iodide electrolyte solution was prepared by dissolving 0.127 g of 0.05 M Iodine (I<sub>2</sub>) in 10 mL of water-free ethylene glycol, then adding 0.83 g of 0.5 M potassium iodide (KI). The electrolyte was inserted

in the cell with a syringe, filling the space between the two electrodes.

**2.4. Measurements.** The absorption spectra of CdS QDs were recorded by PA technique. The light beam from xenon lamp (400 Watt) was focused into the entrance slit of a monochromator (Newport oriel product line model 74125). The output beam of the exit slit was mechanically modulated by an optical chopper (SR540), and focused onto the sample which was mounted carefully inside a PA cell (MTEC Model 300). The sound wave generated from the sample can be subsequently detected as an acoustic signal by a highly sensitive electrical microphone fixed in the PA cell. The PA signal was then amplified by a low noise preamplifier and further processed using a lock-in amplifier (Stanford Research System, Model SR830 DSP). A personal computer was interfaced to the system for automatic data acquisition and analysis.

The PA spectra were compared to those obtained by a regular UV-Vis absorption (JASCO V-670). The particle sizes were estimated directly using TEM and confirmed by PA spectra. The CdS QDSSCs were subjected to the illumination of a solar simulator (ABET technologies, Sun 2000 Solar Simulators, USA) operating at 100 mW/cm<sup>2</sup> (AM 1.5). The current density-voltage ( $J$ - $V$ ) characteristics for CdS QDSSCs of different dipping time were recorded with a Keithley 2400 voltage source/ammeter. The intensity of the incident solar illumination was adjusted to 1 sun condition using a Leybold certified silicon reference solar cell (Model: [57863] Solar cell 2 V/0.3 A STE 4/100).  $J$ - $V$  characteristic curves of QDSSC were recorded at various illumination intensities using attenuators and calibrated by the previous Si reference solar cell. All experiments were carried out under ambient conditions.

## 3. Results and Discussion

**3.1. Optical Absorption Measurements.** The average particle radii of the synthesized CdS QDs were estimated using TEM, which approximately ranged from 1.57 nm for sample a to 1.92 nm for sample d. The TEM images of sample a and d are shown in Figures 1(a) and 1(b), respectively.

The PA spectra for the four samples of CdS QDs (a–d) as a function of the wavelength of the incident beam at a constant modulation frequency of 15 Hz are shown in Figure 2(a). The PA spectra for all samples are normalized using the PA spectrum obtained for carbon black in the allowed region of the used xenon lamp. The absorption edges varies between 394 nm for sample a to 432 nm for sample d. It is easily observed that there is a red shift towards lower energy region with increasing the size. This behavior is attributed to the quantum confinement effect. The calculated energy band gap ( $E_g = hc/\lambda$ ) for the same samples varies between 3.15 eV for sample a to 2.88 eV for sample d. The optical absorption spectra of the same samples in colloidal solution were also obtained by regular UV-Vis absorption and given in Figure 2(b). Although, the UV-Vis. spectra are for samples in colloidal form, and the PA spectra are for powder form, the two spectra gave peaks that are very close.

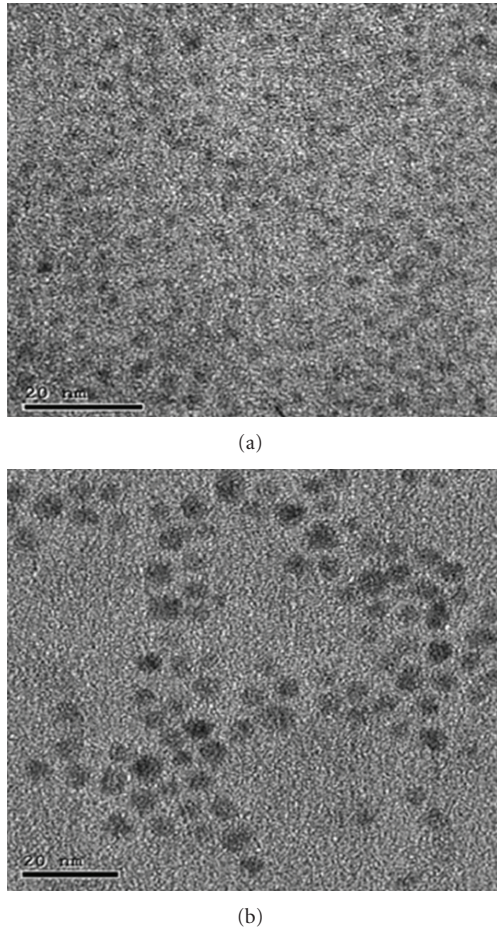


FIGURE 1: (a) TEM micrograph for sample a, and (b) TEM Micrograph for sample d.

The slight difference in the absorption edges positions of CdS QDs between PA and UV-Vis. spectra may be due to the character of the acoustic wave in PA and the photonic character of the UV-Vis.

**3.2. Characterization of CdS QDs Sensitized  $\text{TiO}_2$  Electrodes (The Working Electrode).** The UV-Vis. absorption spectra of the working electrodes for all CdS QDs sizes were recorded for different dipping times (1, 3, 6, 24, and 50 hour). As an example, Figure 3 shows the absorption spectra of CdS QDs (sample d) sensitized  $\text{TiO}_2$  electrodes. It is clearly seen that as the dipping time increases the absorption increases indicating an increased adsorption amount of CdS QDs. Furthermore, a significant shift toward the visible spectra region is also observed.

**3.3. Characterization of CdS QDSSC.** The  $J$ - $V$  characteristics curves of the assembled CdS (sample d) QDSSCs for the five dipped times (1 h, 3 h, 6 h, 24 h, and 50 h) are shown in Figure 4 using  $\text{TiO}_2$  photoelectrodes and  $100 \text{ mW/cm}^2$  from a solar simulator.

The values of  $V_{oc}$ ,  $J_{sc}$ , FF, and  $\eta$  of the assembled QDSSCs at different dipping time are given in Table 1. It is observed

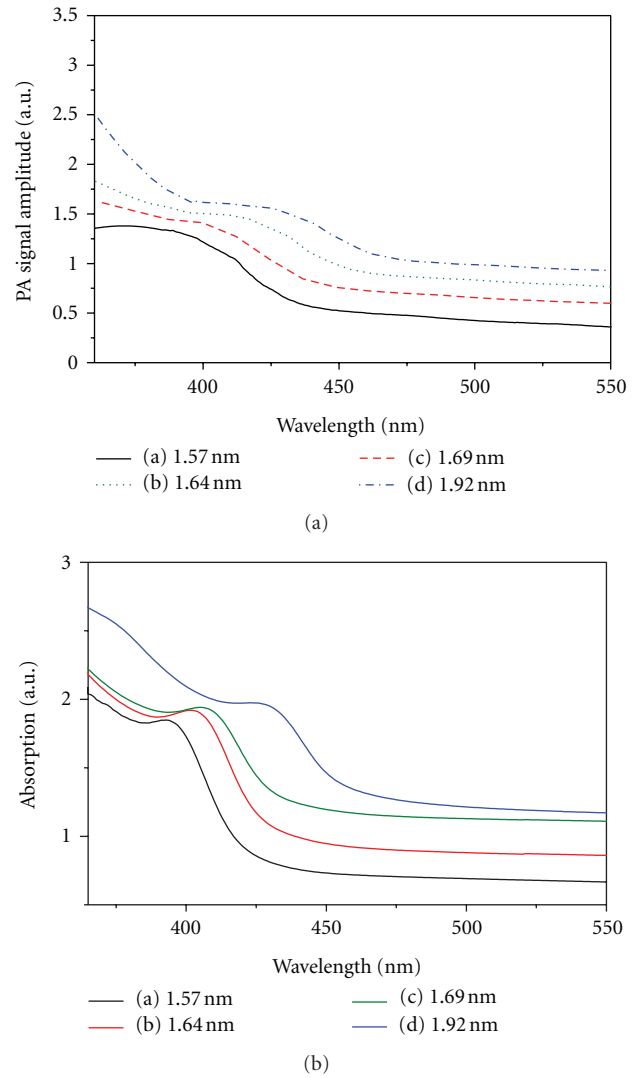


FIGURE 2: (a) normalized PA spectra for the four CdS QDs samples, (b) UV-Vis. absorption spectra for CdS QDs samples.

that both  $J_{sc}$  and  $\eta$  increase as the dipping time increases up to 6 hours, peaking at  $0.67 \text{ mA/cm}^2$  and  $0.18\%$ , respectively. These values lowered down again to  $0.41 \text{ mA/cm}^2$  and  $0.11\%$  for 24 h and  $0.33 \text{ mA/cm}^2$  and  $0.06\%$  for 50 hours dipping time. All other CdS QDs sizes showed the same behavior. These results can be explained in terms of the dipping times. Dipping times greater than 6 hours lead to additional CdSe QDs loading, which, in turn, leads to blocked nanopores in the  $\text{TiO}_2$  layer, causing the reduction of both  $J_{sc}$  and  $\eta$ .

Figure 5 shows the  $J$ - $V$  characteristics of the assembled CdS QDSSCs constructed from different sizes of CdS QDs (with radii 1.57, 1.64, 1.69, and 1.92 nm) at 6 hours dipping time under 1.5 AM illumination from ABET solar simulator. The extracted characteristics parameter are given in Table 2.

It is clearly seen that as CdS QDs size increases, the values of  $J_{sc}$  and  $\eta$  increase. The maximum values of  $J_{sc}$  and  $\eta$  are  $0.67 \text{ mA/cm}^2$  and  $0.18\%$ , respectively, for the biggest

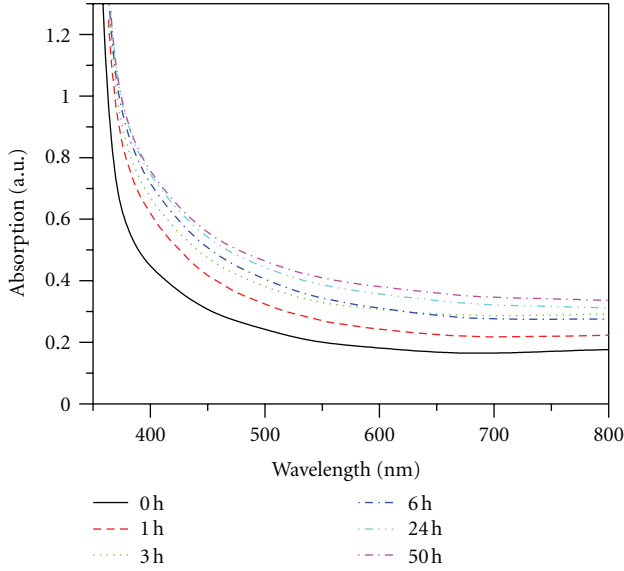


FIGURE 3: UV-Vis. absorption spectra of CdS QDs (sample d) deposited on TiO<sub>2</sub> NPs at 0, 1, 3, 6, 24, and 50 hour dipping time.

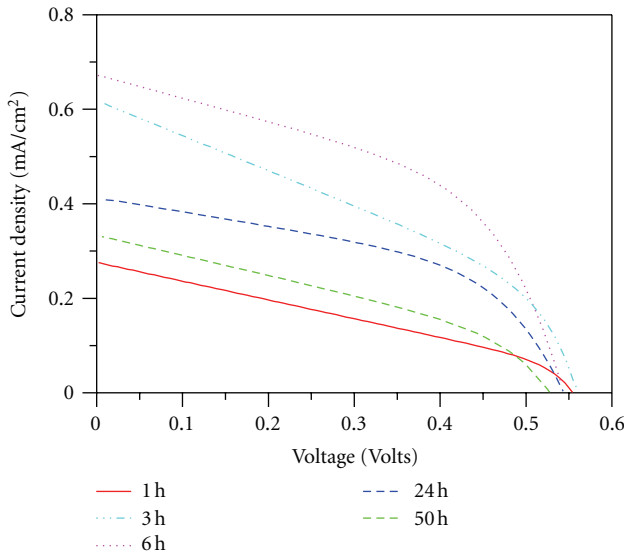


FIGURE 4:  $J$ - $V$  characteristics curves of CdS (sample d) QDSSCs for (a) 1 h, (b) 3 h, (c) 6 h, 24 h, and (d) 50 h dipping time.

TABLE 1:  $J$ - $V$  characteristics parameters of CdS (sample d) QDSSCs for different dipping times.

Dipping time (h)	$V_{oc}$ (Volt)	$J_{sc}$ (mA/cm <sup>2</sup> )	FF	$\eta$ (%)
1	0.56	0.27	0.32	0.05
3	0.56	0.62	0.37	0.13
6	0.54	0.67	0.50	0.18
24	0.54	0.41	0.49	0.11
50	0.53	0.33	0.34	0.06

CdS QDs size (sample d). This result could be explained as follows. Increasing the particle size results in a red shift

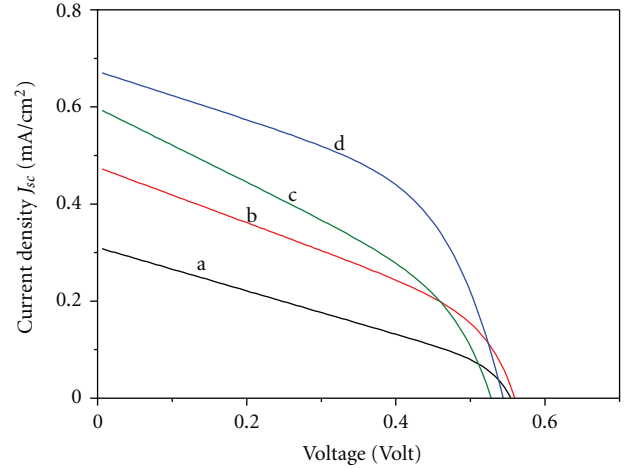


FIGURE 5:  $J$ - $V$  characteristic curve of QDSSCs of CdS QDs radii: (a) 1.57, (b) 1.64, (c) 1.69, and (d) 1.92 nm.

TABLE 2:  $J$ - $V$  characteristics parameters of CdS QDSSCs for different QDs sizes, at 6 hours dipping time, under 1 sun illumination.

CdS QDs size (nm)	QD band gap (eV)	$V_{oc}$ (Volt)	$J_{sc}$ (mA/cm <sup>2</sup> )	FF	$\eta$ (%)
1.57	3.15	0.55	0.31	0.31	0.05
1.64	3.09	0.56	0.47	0.37	0.09
1.69	3.04	0.53	0.60	0.36	0.11
1.92	2.89	0.54	0.67	0.50	0.18

and thus causes relatively high absorption of the incident photon from solar spectrum. Therefore, CdS QDs of radius 1.92 nm (correspond to 432 nm) harvest more visible photon than the other particles sizes. Furthermore, It is seen that  $V_{oc}$  is independent on CdS QDs size, since the electrons injected quickly from the CBM of CdS QDs to the lowest CB energy of TiO<sub>2</sub> NPs, indicating that the CB level of TiO<sub>2</sub> NPs and the VB of the electrolyte dictate  $V_{oc}$  of the assembled QDSSCs. Additionally, DA technique which we used to deposit CdS QDs onto TiO<sub>2</sub> NPs lead to pin directly the CdS QDs bands to that of TiO<sub>2</sub> NPs without any barriers, which causes a direct electronic interaction between the two semiconductor materials (CdS QDs and TiO<sub>2</sub> NPs). So, DA technique minimizes the electrons' injection time from CBM of CdS QDs to that of TiO<sub>2</sub> NPs.

The performance of the assembled CdS (sample d) QDSSCs with various intensities of solar illumination (from 0 to 100% sun) are given in Figure 6. It is seen that as the intensity of the incident light increases, the measured  $J_{sc}$  increases linearly due to increased injected electrons. The approximately constant value of  $V_{oc}$  indicate the relative sensitivity of CdS QDSSCs that is prepared by DA method.

## 4. Conclusions

The nondestructive PA technique has been used to study the optical absorption spectra of CdS QDs of different sizes. The spectra shifted to lower energy region with increasing

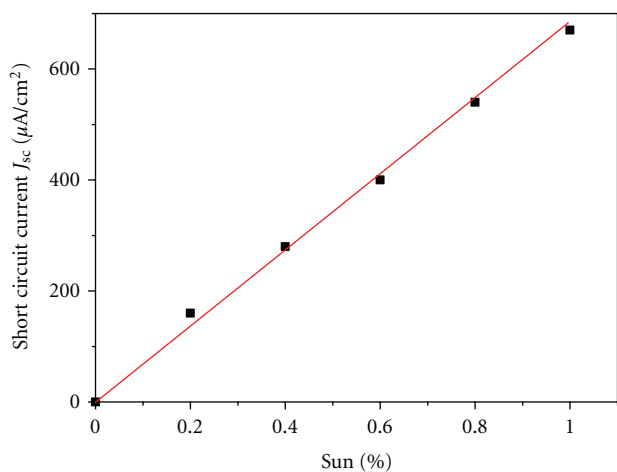


FIGURE 6: short circuit current density ( $J_{sc}$ ) versus percentage of sun.

the particle size. The PA spectra were compared with regular UV-Vis absorption which gives comparable results. These CdS QDs of different sizes were deposited onto  $\text{TiO}_2$  NPs using DA technique by varying dipping time (0 to 50 hours) to serve as a sensitizer for photovoltaic cell. Our results show that DA technique is a suitable method to adsorb CdS QDs onto  $\text{TiO}_2$  nanoparticles up to 50 hours without use of linkers. The values of  $J_{sc}$  and  $\eta$  increase as the QDs size increases. Such an increase is mostly attributed to the consistence with the incident solar intensity spectrum. Furthermore, as the intensity of the incident solar light increases,  $J_{sc}$  increases linearly, indicating greater sensitivity of CdS QDSSCs.

## Acknowledgments

The authors wish to thank Taif University for the Grant Research no. (1/432/1110). The Quantum Optics Research Group (QORG) at Taif University is also thanked for their assistance during this work.

## References

- [1] B. Pejova, A. Tanuševski, and I. Grozdanov, "Semiconducting thin films of zinc selenide quantum dots," *Journal of Solid State Chemistry*, vol. 177, no. 12, pp. 4785–4799, 2004.
- [2] P. K. Khanna and N. Singh, "Light emitting CdS quantum dots in PMMA: synthesis and optical studies," *Journal of Luminescence*, vol. 127, no. 2, pp. 474–482, 2007.
- [3] D. Patidar, K. S. Rathore, N. S. Saxena, K. Sharma, and T. P. Sharma, "Energy band gap and conductivity measurement of CdSe thin films," *Chalcogenide Letters*, vol. 5, no. 2, pp. 21–25, 2008.
- [4] D. K. Dwivedi, Dayashankar, and M. Dubey, "Synthesis, characterization and electrical properties of ZnTe nanoparticles," *Journal of Ovonic Research*, vol. 5, no. 1, pp. 35–41, 2009.
- [5] P. Raji, C. Sanjeeviraja, and K. Ramachandran, "Thermal and structural properties of spray pyrolysed CdS thin film," *Bulletin of Materials Science*, vol. 28, no. 3, pp. 233–238, 2005.
- [6] F. Semendy and U. S. Army Research Laboratory, *Colloidal CdTe Nanocrystals Synthesis and Characterization*, Army Research Laboratory, Adelphi, Md, USA, 2008.
- [7] P. Guyot-Sionnest, "Colloidal quantum dots," *Comptes Rendus Physique*, vol. 9, no. 8, pp. 777–787, 2008.
- [8] T. A. El-Brolossy, S. Abdallah, T. Abdallah, M. B. Mohamed, S. Negm, and H. Talaat, "Photoacoustic characterization of optical and thermal properties of CdSe quantum dots," *European Physical Journal*, vol. 153, no. 1, pp. 365–368, 2008.
- [9] S. D. George, S. Augustine, E. Mathai, P. Radhakrishnan, V. P. N. Nampoori, and C. P. G. Vallabhan, "Effect of Te doping on thermal diffusivity of  $\text{Bi}_2\text{Se}_3$  crystals: a study using open cell photoacoustic technique," *Physica Status Solidi (a)*, vol. 196, no. 2, pp. 384–389, 2003.
- [10] M. A. Gonzalez-T, A. Cruz-Orea, M. de L. Albor-A, and F. de L. Castillo-A, "Thermal characterization and determination of recombination parameters in CdTe films on glass substrates by using open photoacoustic cell technique," *Thin Solid Films*, vol. 480–481, pp. 358–361, 2005.
- [11] K. Prabakar, H. Seo, M. Son, and H. Kim, "CdS quantum dots sensitized  $\text{TiO}_2$  photoelectrodes," *Materials Chemistry and Physics*, vol. 117, no. 1, pp. 26–28, 2009.
- [12] Y. Xie, S. H. Yoo, C. Chen, and S. O. Cho, "Ag<sub>2</sub>S quantum dots-sensitized  $\text{TiO}_2$  nanotube array photoelectrodes," *Materials Science and Engineering: B*, vol. 177, no. 1, pp. 106–111, 2012.
- [13] W. Lee, S. K. Min, V. Dhas, S. B. Ogale, and S. H. Han, "Chemical bath deposition of CdS quantum dots on vertically aligned ZnO nanorods for quantum dot-sensitized solar cells," *Electrochemistry Communications*, vol. 11, no. 1, pp. 103–106, 2009.
- [14] A. Tubtimtae, K. L. Wu, H. Y. Tung, M. W. Lee, and G. J. Wang, "Ag<sub>2</sub>S quantum dot-sensitized solar cells," *Electrochemistry Communications*, vol. 12, no. 9, pp. 1158–1160, 2010.
- [15] I. Barceló, T. Lana-Villarreal, and R. Gómez, "Efficient sensitization of ZnO nanoporous films with CdSe QDs grown by successive Ionic layer adsorption and reaction (SILAR)," *Journal of Photochemistry and Photobiology A*, vol. 220, no. 1, pp. 47–53, 2011.
- [16] J. H. Bang and P. V. Kamat, "Quantum dot sensitized solar cells. a tale of two semiconductor nanocrystals: CdSe and CdTe," *ACS Nano*, vol. 3, no. 6, pp. 1467–1476, 2009.
- [17] L. Mora-Ser'o, S. Giménez, T. Moehl et al., "Factors determining the photovoltaic performance of a CdSe quantum dot sensitized solar cell: the role of the linker molecule and of the counter electrode," *Nanotechnology*, vol. 19, no. 42, Article ID 424007, 2008.
- [18] S. Rühle, M. Shalom, and A. Zaban, "Quantum-dot-sensitized solar cells," *ChemPhysChem*, vol. 11, no. 11, pp. 2290–2304, 2010.
- [19] A. Salant, M. Shalom, I. Hod, A. Faust, A. Zaban, and U. Banin, "Quantum dot sensitized solar cells with improved efficiency prepared using electrophoretic deposition," *ACS Nano*, vol. 4, no. 10, pp. 5962–5968, 2010.
- [20] N. J. Smith, K. J. Emmett, and S. J. Rosenthal, "Photovoltaic cells fabricated by electrophoretic deposition of CdSe nanocrystals," *Applied Physics Letters*, vol. 93, no. 4, Article ID 043504, 2008.
- [21] A. Kongkanand, K. Tvrđy, K. Takechi, M. Kuno, and P. V. Kamat, "Quantum dot solar cells. Tuning photoresponse through size and shape control of CdSe- $\text{TiO}_2$  architecture," *Journal of the American Chemical Society*, vol. 130, no. 12, pp. 4007–4015, 2008.
- [22] D. R. Pernik, K. Tvrđy, G. J. Radich, and P. V. Kamat, "Tracking the adsorption and electron injection rates of CdSe quantum dots on  $\text{TiO}_2$ : linked versus direct attachment," *The Journal of Physical Chemistry C*, vol. 115, no. 27, pp. 13511–13519, 2011.

- [23] P. V. Kamat, "Quantum dot solar cells. Semiconductor nanocrystals as light harvesters," *Journal of Physical Chemistry C*, vol. 112, no. 48, pp. 18737–18753, 2008.
- [24] S. Giménez, I. Mora-Seró, L. Macor et al., "Improving the performance of colloidal quantum-dot-sensitized solar cells," *Nanotechnology*, vol. 20, no. 29, Article ID 295204, 2009.
- [25] N. Guijarro, T. Lana-Villarreal, I. Mora-Seró et al., "CdSe quantum dot-sensitized TiO<sub>2</sub> electrodes: effect of quantum dot coverage and mode of attachment," *The Journal of Physical Chemistry C*, vol. 113, no. 10, pp. 4208–4214, 2009.
- [26] L. Manna, E. C. Scher, and A. P. Alivisatos, "Synthesis of soluble and processable rod-, arrow-, teardrop-, and tetrapod-shaped CdSe nanocrystals," *Journal of the American Chemical Society*, vol. 122, no. 51, pp. 12700–12706, 2000.
- [27] G. Syrokostas, M. Giannouli, and P. Yianoulis, "Effects of paste storage on the properties of nanostructured thin films for the development of dye-sensitized solar cells," *Renewable Energy*, vol. 34, no. 7, pp. 1759–1764, 2009.



**Hindawi**

Submit your manuscripts at  
<http://www.hindawi.com>

